SCIENTIFIC REPORTS

SUBJECT AREAS:
ELECTRONIC MATERIALS AND DEVICES
APPLIED PHYSICS
MATERIALS PHYSICS
ELECTROCHEMISTRY

Received
30 May 2012

Accepted
7 September 2012

Published
25 September 2012

Correspondence and requests for materials should be addressed to Y.J. (yjun@unist.ac.kr) or Y.W.P. (ywpark@phya.snu.ac.kr)

* These authors contributed equally to this work.

N-type graphene induced by dissociative H_2 adsorption at room temperature

Byung Hoon Kim[1]*, Sung Ju Hong[2]*, Seung Jae Baek[2], Hu Young Jeong[3], Noejung Park[1], Muyoung Lee[1], Sang Wook Lee[4], Min Park[2], Seung Wan Chu[2], Hyeon Suk Shin[1], Jeongmin Lim[1], Jeong Chul Lee[5], Yongseok Jun[1] & Yung Woo Park[2]

[1]Interdisciplinary School of Green Energy, KIER-UNIST Advanced Center for Energy, Ulsan National Institute of Science and Technology (UNIST), Ulsan 689-798, Republic of Korea, [2]Department of Physics and Astronomy and Department of Nano Science and Technology, Seoul National University, Seoul 151-747, Republic of Korea, [3]UNIST Central Research Facility and School of Mechanical and Advanced Materials Engineering, Ulsan National Institute of Science and Technology (UNIST), Ulsan 689-798, Republic of Korea, [4]Division of Quantum Phases and Devices, School of Physics, Konkuk University, Seoul 143-701, Republic of Korea, [5]KIER-UNIST Advanced Center for Energy, Korea Institute of Energy Research, Daejeon, 305-343, Republic of Korea.

Studies of the interaction between hydrogen and graphene have been increasingly required due to the indispensable modulation of the electronic structure of graphene for device applications and the possibility of using graphene as a hydrogen storage material. Here, we report on the behaviour of molecular hydrogen on graphene using the gate voltage-dependent resistance of single-, bi-, and multi-layer graphene sheets as a function of H_2 gas pressure up to 24 bar from 300 K to 345 K. Upon H_2 exposure, the charge neutrality point shifts toward the negative gate voltage region, indicating n-type doping, and distinct Raman signature changes, increases in the interlayer distance of multi-layer graphene, and a decrease in the *d*-spacing occur, as determined by TEM. These results demonstrate the occurrence of dissociative H_2 adsorption due to the existence of vacancy defects on graphene.

Graphene has been regarded as the successor of silicon in the electronics industry due to its remarkably high carrier mobility, transparency, anomalous quantum Hall effect[1–4], and exceptionally high Young's modulus[5]. However, the electronic structure of graphene, which features gap opening and *n*- and *p*-type properties, must be controlled to achieve this demand. One of the methods used to control the properties of graphene is hydrogenation. Hydrogenated graphene, known as graphane, is obtained from hydrogen plasma and shows a hole-doping effect, a reversible insulating state, and the disappearance of the quantum Hall effect[6–10]. Along with the hydrogenation of graphene, considerable attention has been paid to the adsorption behaviour of molecular hydrogen on graphitic materials, as well as the interaction between atomic hydrogen and graphene, because multilayered graphene has been proposed as a good candidate for hydrogen storage[11–15]. For physisorption, the attraction between H_2 and graphene occurs via overlapping of the σ molecular orbital of H_2 with the electrons in the π state of graphene, with no charge transfer[16]. However, the dissociative adsorption of hydrogen molecules on a graphite surface with vacancies[17] and at the armchair edge of graphite[18] has been theoretically suggested. Herein, we report on the dissociative adsorption of hydrogen with gate-voltage (V_G)-dependent current variations of single-, bi-, and multi-layer graphene (SLG, BLG, and MLG, respectively) as a function of H_2 gas pressure from vacuum (approximately 10^{-6} Torr) to 24 bar at temperatures $T \geq 300$ K. As the H_2 gas pressure increases, the charge neutrality point (CNP) shifts toward the negative V_G region (*n*-doping). This charge neutrality point does not return to the origin, even after degassing is performed (vacuum and heating at 393 K). Long exposure times and high temperatures in a H_2 atmosphere enhance the *n*-doping effect. H_2 exposure leads to the development of defect-related *D* (approximately 1350 cm^{-1}) and *D*' (approximately 1620 cm^{-1}) peaks and a peak corresponding to the C-H bond (approximately 2932 cm^{-1}), a blueshift in the *G* peak, and a change in stacking order deleted by the variation in the 2*D* peak, as observed in Raman spectra. An increase in the interlayer distance of MLG was observed by atomic force microscopy (AFM) and X-ray diffraction (XRD). Transmission electron microscopy (TEM) showed in-plane compression after H_2 exposure. We also found that the extent of CNP variation is related to the number of graphene layers present. These results show that dissociative H_2 adsorption is mainly caused by the vacancy defects of graphene, thus providing a better understanding of the interaction between the H_2 molecule and graphene and offering evidence of the possibility of accessing more potential degrees of freedom for electronic applications using graphene.

Results

The V_G-dependent resistance (R) of SLG (Fig. 1a), BLG (Fig. 1b), and MLG (Fig. 1c) as a function of H_2 pressure up to 24 bar was measured. We observed a shift in the CNP toward the negative V_G region in a H_2 atmosphere. This shift indicates n-type behaviour, which becomes prominent as the layer number increases. Upon exposure to H_2 (1 bar), the graphene sheets seemed to be doped by electrons. By further exposing the graphene sheets to H_2 molecules, a high H_2 pressure enhances this effect. This effect was also observed in the V_G-dependent current-voltage (I-V) characteristics (Supplementary Fig. S2). Upon H_2 exposure, (1) the maximum resistance (R_M) increases in BLG and MLG but the R_M of SLG decreases, and (2) far from V_G at the CNP (V_{CNP}), R in the $V_G < V_{CNP}$ region increases while R in the $V_G > V_{CNP}$ region decreases. The main carriers are holes and electrons at $V_G < V_{CNP}$ and $V_G > V_{CNP}$, respectively. Hence, the n-doping effect induced by H_2 exposure produces result (2) mentioned above. For result (1), the increase in R_M in BLG and MLG can be understood with respect to the increase in the impurity carrier density[19] but not for the reduction of R_M in SLG. Hence, we tentatively suggest that the reduction in R_M results from competition between the residual carrier density and the impurity carrier density, i.e., H_2 exposure contributes more to the increase in the residual carrier density than the impurity density in SLG.

Desorption occurred as the H_2 pressure was reduced, as shown in the right panels of Figure 1, and only a slight shift in V_{CNP} to the negative V_G region was detected, which will be discussed later. More interestingly, even after applying a high vacuum (approximately 10^{-6} Torr) at 393 K, the CNP did not return to the original value obtained

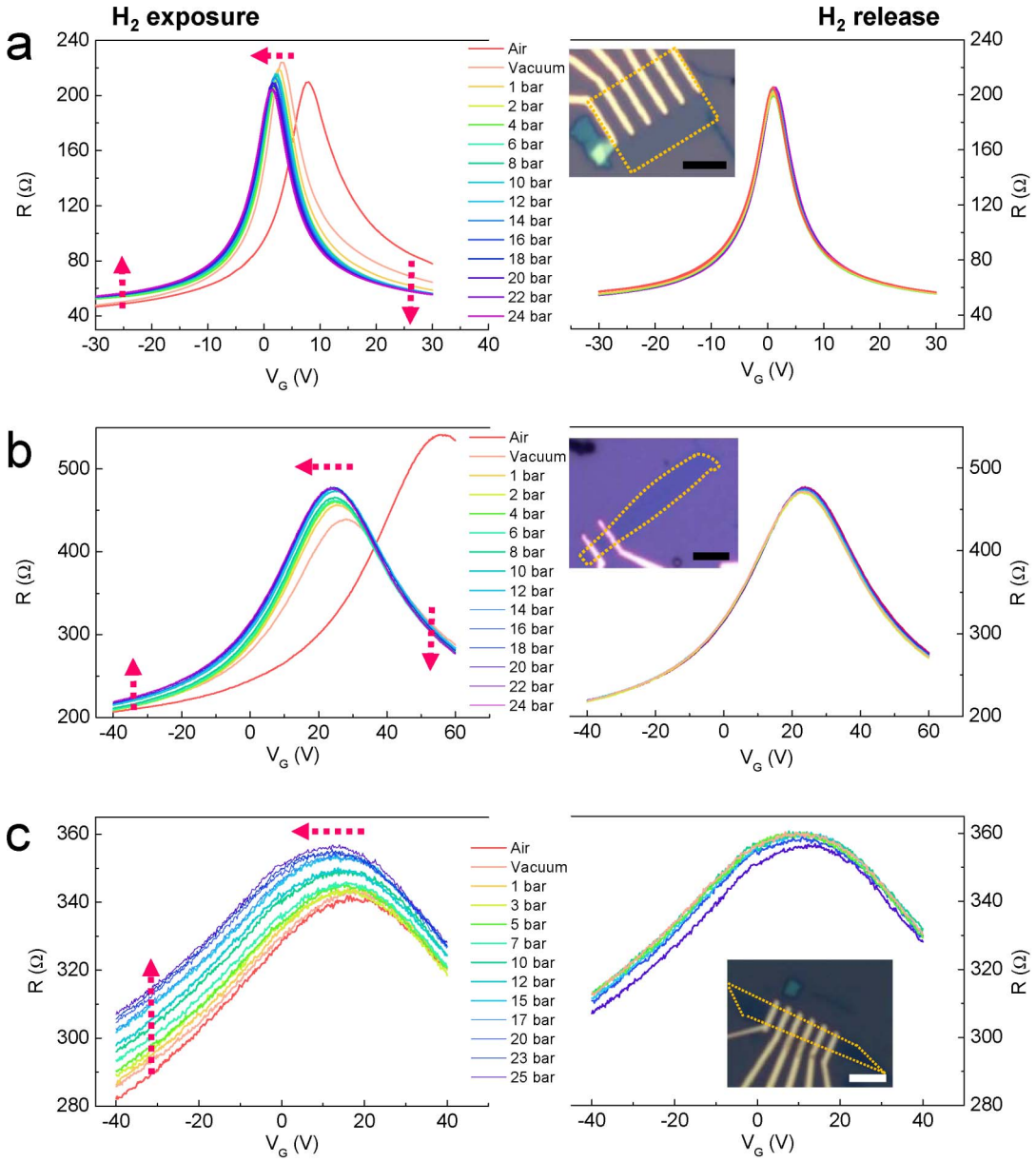

Figure 1 | V_G-dependent R as a function of H_2 pressure for (a) SLG, (b) BLG, and (c) MLG. At H_2 pressure = 0 (vacuum), all graphene samples show the standard ambipolar field effect and the CNP broadens as the layer number increases. Upon H_2 exposure (left panels), the CNPs of all graphene samples shift toward the negative V_G region. The shift becomes larger with increasing layer number. In SLG, the maximum resistance, R_M, decreases, but it increases in BLG and MLG. The decrease in R_M may be a characteristic fingerprint of SLG. An increase and decrease in R for $V_G \ll V_{CNP}$ and for $V_G \gg V_{CNP}$ are observed in SLG and BLG. In the case of MLG, this behaviour may be observed over a wide-range V_G sweep. During the release process (right panel), the same propensity is shown but is very small. The insets show optical microscopy images for each graphene sample. The scale bar is 5 μm.

before H_2 exposure. This result suggests dissociative H_2 adsorption of graphene. The variation in CNP as the H_2 pressure was increased and decreased is clearly shown in Supplementary Fig. S3.

With regard to graphene, the attached hydrogen atoms can be considered impurities that exert the *n*-doping effect on graphene. Raman spectroscopy can provide information regarding this type of defect. The *D* peak near 1350 cm^{-1} is a breathing mode of A_{1g} symmetry, which is ascribed to the presence of disorder. The *G* peak near 1580 cm^{-1} is the in-plane stretching mode of sp^2 carbon[20]. The *G* band is blueshifted by the variation in charge density[21]. Development of the *D* peak and a blueshift in the *G* peak were observed after H_2 exposure (Fig. 2a). Before H_2 exposure, the *G* bands were located at 1586 cm^{-1}, 1582 cm^{-1}, and 1583 cm^{-1} for SLG, BLG, and MLG, respectively. After exposing the graphene to a H_2 pressure of 24 bar, these peaks were shifted to 1591 cm^{-1}, 1584 cm^{-1}, and 1588 cm^{-1}, respectively, and a *D* peak developed near 1350 cm^{-1} (for BLG, the *D* peak can be more clearly observed in Supplementary Fig. S4). The 2*D* band (approximately 2700 cm^{-1}) for SLG and BLG showed little change, but this was not the case for MLG. In the Raman spectra of graphene, the 2*D* band was very sensitive to the stacking order of the graphene layers. As a result, turbostratic graphite, which lacks a stacking order, can be considered 2-dimensional (2-D) graphite[22]. The 2*D* band of MLG consisted of two sub-bands at 2686.52 ± 0.60 cm^{-1} and 2720.91 ± 0.16 cm^{-1} (Fig. 2b). These peaks are ascribed to contributions from 2-D graphite and the highly oriented 3-D structure of graphite, respectively[23]. Before H_2 exposure, the peak (P_1) corresponding to 2-D graphite was smaller than the peak (P_2) originating from the 3-D graphitic structure. After H_2 exposure, P_1 increases, but P_2 decreases. This is also observed in graphene grown by CVD without electrodes (see Supplementary Fig. S4). Note that the development of the peak at approximately 2930 cm^{-1} was observed in both MLG obtained by mechanical exfoliation and that produced by CVD growth (green arrows in Figs. 2b and 2c). This peak corresponds to the sp^3 C-H stretching mode[24]. The C-H bending mode, which occurs at approximately 1330 cm^{-1}, overlapped with the *D* peak[24,25]. To confirm the development of these peaks, we measured the H_2 pressure-dependent Raman spectra of CVD graphene (Fig. 2c). Upon reaching a H_2 pressure of 10 bar, the *D* and *D*' (approximately 1620 cm^{-1}) peaks increased and the peak for the C-H stretching mode at 2930 cm^{-1} developed. As the H_2 pressure was increased to 20 bar, the *D* and C-H peaks were enhanced. After evacuation at 393 K for 3 hr, the intensities of the

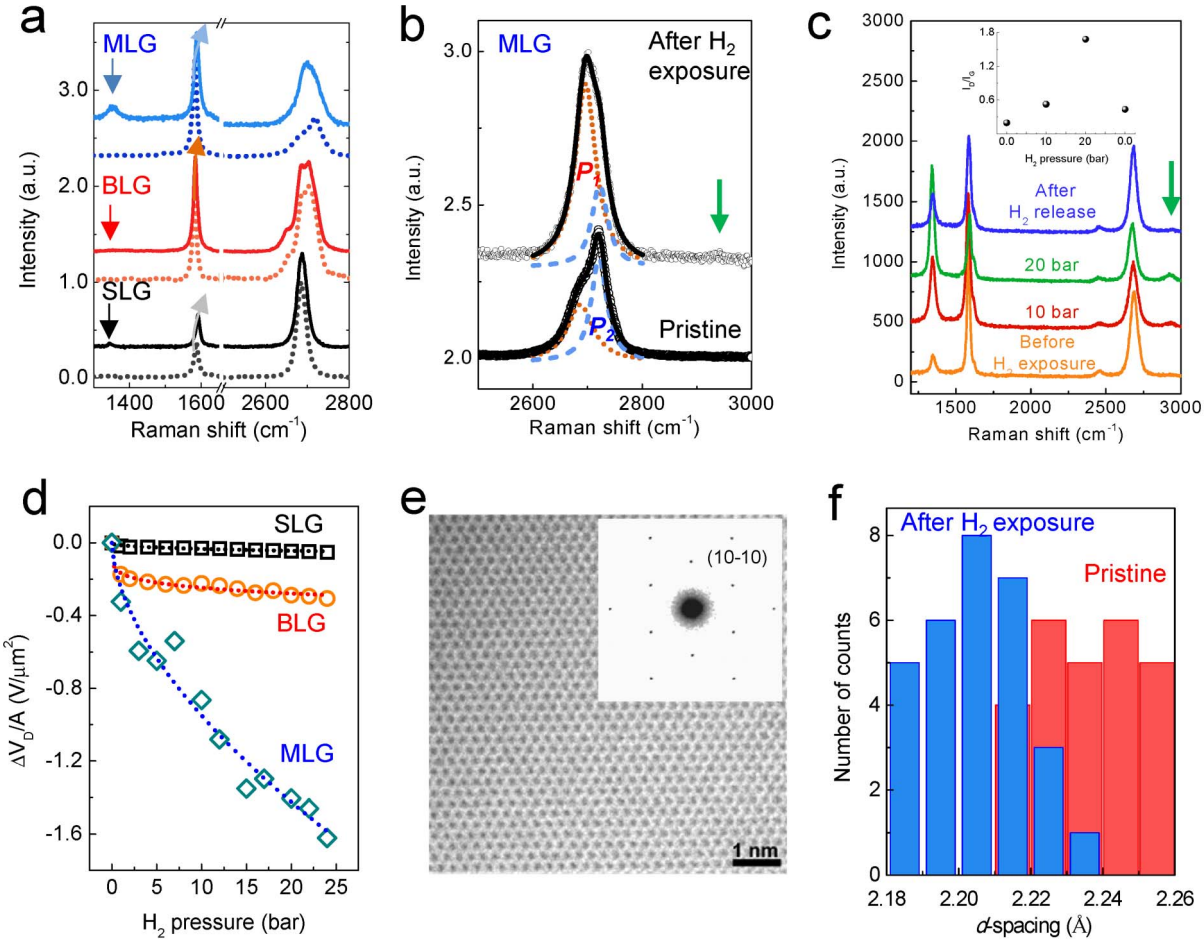

Figure 2 | Dissociative H_2 adsorption. (a) Raman spectra for SLG, BLG, and MLG before (dotted line) and after H_2 exposure. Broadening and a blueshift of the *G* band (sp^2 carbon) occur, and the *D* band near 1350 cm^{-1} (sp^3 carbon) develops due to H_2 exposure. (b) A close view of the variation in the 2*D* band of MLG. The small peak at approximately 2930 cm^{-1} corresponds to the C-H bond (green arrow). (c) H_2 pressure-dependent Raman spectroscopy of the CVD graphene. The defect evolution (I_D/I_G ratio) is depicted in the inset. Two zero values of H_2 pressure are observed, one before H_2 exposure (first one) and one after evacuation (left one). The peak for the C-H bond is clearly shown in the CVD graphene. (d) The variation in V_{CNP} increases as the number of graphene layers increases. We chose V_{CNP} at the highest pressure of 24 bar in this study with the assumption that hydrogen is almost saturated on and within the graphene at this pressure. (e) TEM image and ED patterns for graphene after H_2 exposure. The carbon honeycomb lattice is clearly shown. (f) A histogram shows the *d*-spacings (10-10) for thirty different regions of graphene before (red) and after (blue) H_2 exposure. The averaged *d*-spacings for pristine and hydrogen-chemisorbed graphenes are 2.22 ± 0.016 Å and 2.20 ± 0.014 Å, respectively.

two peaks were weakened, but the peaks were not identical to those obtained before H_2 exposure. This indicates that a small degree of C-H bonding remains even after evacuation, which is similar to the result observed for the V_G-dependent R after the release process. The inset of Figure 2c shows the change in the I_D/I_G ratio as a function of the H_2 pressure. I_D/I_G increased with the increase in H_2 pressure and then decreased after evacuation. The results obtained from Raman study reveals that the attached H atoms dissociated by graphene produce an incommensurate structure such as turbostratic graphite.

By AFM, we observed an increase in the thickness of MLG from 3.2 ± 0.52 nm to 7.2 ± 0.82 nm after H_2 exposure (Supplementary Fig. S5). An increase in the interlayer distance was also observed in the graphene prepared by CVD methods. Before H_2 exposure, very small XRD peaks near $2\theta = 15.8^\circ$ and 26.5° (3.36 Å) were observed. The small peaks are attributed to the few-layer graphene grown by CVD. Upon H_2 exposure, even at 1 bar of H_2 pressure, the peak near $2\theta = 15.8^\circ$ (5.61 Å) became larger and shifted to a lower angle: 5.99 Å at 10 bar and 6.16 Å at 20 bar, indicating that the interlayer distance of few-layer graphene increased (Supplementary Fig. S4).

The impurity carrier density is proportional to the ΔV_{CNP} induced by H_2 exposure[26]. To investigate the effect of the impurity carrier density for these three types of graphene, we obtained values for $\Delta V_{CNP}/A$ (Fig. 2d). A is the area of the three types of graphene between two electrodes. Increasing the number of graphene layers leads to an increase in ΔV_{CNP}. At 24 bar, $\Delta V_{CNP}/A$= -0.05189 V/μm^2 for SLG, -0.3065 V/μm^2 for BLG, and −1.6216 V/μm^2 for MLG. If we assume that the same number of dissociated hydrogen atoms is attached to each graphene layer, the specific $\Delta V_{CNP}/A$ relationship for each of the three graphenes can be determined. Considering the $\Delta V_{CNP}/A$ of SLG (−0.05189 μm^{-2}), the $\Delta V_G/A$ due to the interspace of BLG becomes −0.2546 V/μm^2, which shows that hydrogen atoms are attached to not only the edge but also the central region of the graphene. The MLG used in the measurement has seven layers, indicating that it has six BLG interspaces and one layer of SLG (AFM images in Supplementary Fig. S5). Therefore, a variation of −1.5796 V/μm^2 can be estimated by the variation in V_{CNP} for SLG and the interspace of BLG. This value is similar to that obtained for the variation in the CNP in MLG (1.6216 V/μm^2, the small discrepancy between the two values may be due to the error in the height obtained by AFM). This similarity indicates that the shift in CNP toward the n-type carrier regime is due to the graphene itself and not other effects such as dielectric screening caused by hydrogen molecules between the graphene and the SiO_2 substrate[27]. An increase in interlayer distance at high H_2 pressure[13] is theoretically expected, and an enhancement in the peak near $2\theta = 15^\circ$ in the XRD patterns of CVD graphene (see Supplementary Fig. S4) shows that the structure of hydrogen molecule-intercalated MLG can be interpreted as second-stage structures such as graphite bromine lamellar compounds[28]. However, because electrical charge cannot be transferred from hydrogen molecules to graphene[16], the physisorption of H_2 molecules can be attributed to the increase in the interlayer distance, but this is not the reason for the n-type doping of graphene.

Strong evidence for chemisorption was obtained from TEM images of single-layer graphene grown by CVD methods (Figs. 2e and 2f). Structural modulation was indicated by the electron-diffraction (ED) patterns for 30 different regions of a graphene sample obtained before and after H_2 exposure. The d-spacings of pristine graphene were distributed over distances ranging from 2.197 to 2.256 Å. In the case of H_2-exposed graphene, the d-spacing was reduced (2.181–2.232 Å), indicating that in-plane compression occurs due to the chemical bonding of hydrogen[6].

Thus far, we have investigated the properties of graphene upon H_2 exposure at 300 K. The results indicate that the dissociation barrier of H_2 is reduced on graphene. Accordingly, the V_G-dependent R of MLG at constant H_2 pressure (10 bar) was measured with increasing temperature up to 340 K (Fig. 3). Upon exposing the graphene to 10 bar of H_2 pressure, the CNP shifted from 7.40 V to 6.80 V and then remained constant up to T = 310 K. Beyond T = 315 K, the CNP started to shift again (6.65 V at 315 K and 6.30 V at 320 K) and was slightly enhanced at 325 K (5.80 V at 325 K). At $T > 330$ K, the CNP changes significantly from 5.30 V to 1.20 V at 340 K (Fig. 3a). The dissociation of H_2 was much more favourable at high temperature. This finding indicates that the probability of overcoming the dissociation barrier increases, even for a small thermal energy. During cooling, we observed an interesting feature. Figure 3b shows the variation in CNP as a function of time at 330 K. Although T decreased from 340 K to 330 K, the CNP continuously shifted to −4.1 V (70 min elapsed after the measurement at 340 K). With increasing time, the CNP decreased to −7.9 V at a constant temperature T = 330 K. This shift is natural because the thermal energy at a temperature of 330 K exceeds the dissociation barrier, as shown in Figure 3a. Further shifts in V_G during the release process (Fig. 1 and Supplementary Fig. S3) can be understood in the same way. The CNP continued to shift up to 320 K, but it remained constant beyond T = 310 K (Fig. 3c). The CNPs at 295 K also remained unchanged during evacuation (dotted box in Figs. 3c and 3d). However, heat treatment at 393 K in vacuum for 3 hr caused the CNP to return to approximately its original value (6.8 V). The variation in CNP with decreasing temperature is summarised in Figure 3e.

The same experiment with a different MLG sample was performed for a long exposure time (t) and up to a slightly higher temperature (345 K). Before H_2 exposure, measurements of the V_G-dependent R as a function of T were carried out. The CNP was observed to remain constant up to 345 K (see Supplementary Fig. S6). Upon H_2 exposure, an n-doping effect was also observed. However, the shift in CNP and the decrease in hole mobility became significant compared with the results described in Figure 3, as is clearly shown in Figure 4a. Although $\Delta V_{CNP}/\Delta t$ increased as the temperature increased, $\Delta V_{CNP}/\Delta t$ seemed to saturate at each temperature at even longer times, which implies that both sufficient time and high temperature are necessary to enhance the n-doping effect. As a result, the hole mobility strongly decreased at 345 K after 750 min (Fig. 4b). This behaviour was maintained at 295 K. However, although the ambipolarity is recovered, the current level does not return to its original value in air after heating in a vacuum due to the re-adsorption of admolecules such as O_2 and H_2O in air. If a desorption process (heating in vacuum) is not performed, the CNP moves toward the positive V_G region and is then saturated, i.e., the n-type behaviour is maintained even in air (Supplementary Fig. 7).

Discussion

The dissociative H_2 adsorption barrier on graphite is approximately 3.3 eV[29]. Although this barrier appears prohibitive, dissociation can occur in particular cases. If a hydrogen molecule approaches a vacancy defect on a graphene surface, the molecule becomes largely polarised and finally dissociates[17]. At the edge of graphite, the energy barrier is reduced, causing dissociative adsorption[18,30]. Other possible factors for dissociative H_2 adsorption, including electric fields[31] and mechanical stress[32], have been suggested. In the present study, the C–H bonding of CVD graphene was clearly detected compared with that of mechanically exfoliated graphene. The results show that vacancy defects promote dissociative adsorption because graphene grown by CVD methods has more structural defects than mechanically exfoliated graphene[33].

H molecules dissociated on graphene can break C=C double bonds in the structure of graphene. Consequently, two unpaired electrons are produced. An unpaired electron participates in the formation of a C-H bond, and the other is delocalised[34–37]. This delocalised electron induces an n-type doping effect on graphene.

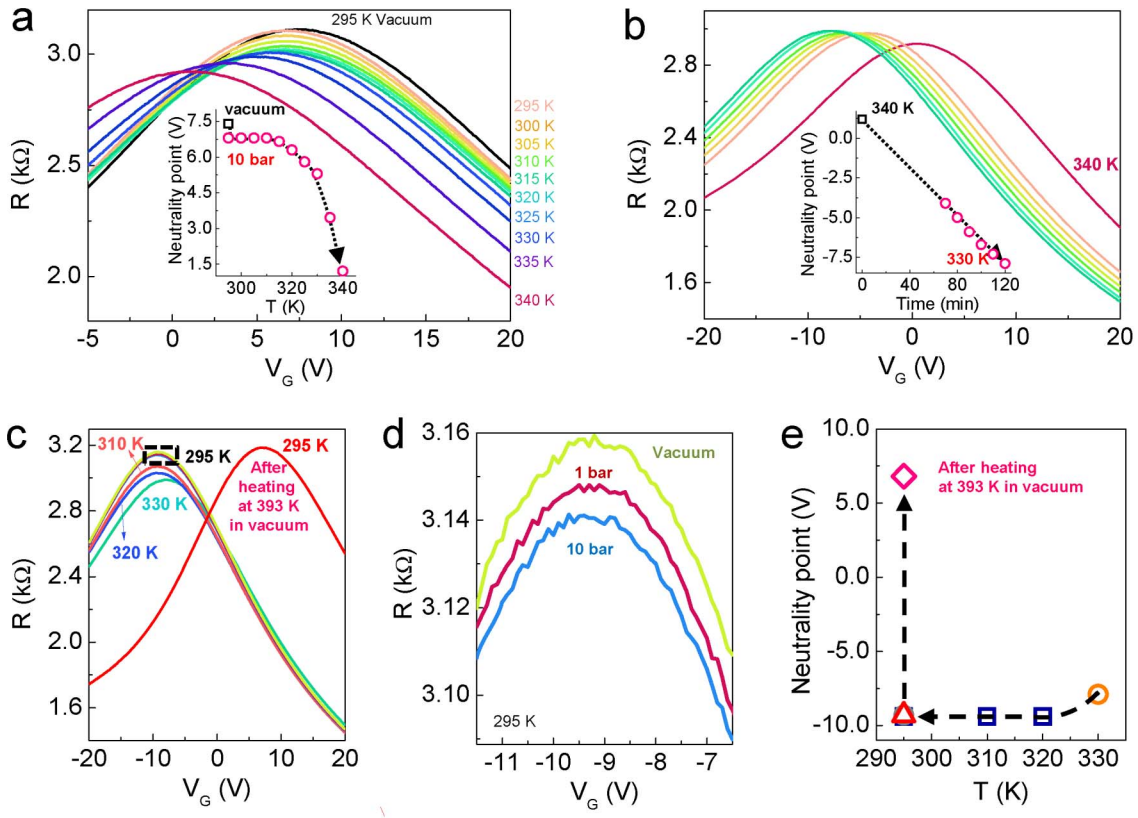

Figure 3 | V_G-dependent R as a function of temperature for MLG at 10 bar of H_2 pressure. MLG samples were used to clarify the *n*-doping effect. (a) Upon exposing the graphene to 10 bar of H_2 at 295 K, the CNP shifts toward the negative V_G region. As the temperature increases up to 310 K, the CNP remains nearly constant. In fact, it shifts but cannot be defined because of the resolution (a V_G sweep interval of 50 mV). Beyond 315 K, the CNP shifts again, and the variation in CNP increases with temperature up to 340 K. (b) During the cooling process, we set the temperature to 330 K. As the exposure time increases, the CNP continuously shifts along the same direction and R_M increases slightly. The insets of (a) and (b) clearly show the variation in the CNP. (c) The shift is maintained down to 320 K but not below 310 K. (d) At 295 K, although the H_2 pressure is released, no shift in the CNP is observed. (e) The variation in the CNP during the release process is depicted.

In addition, we can rule out other possibilities for *n*-doping on graphene in a H_2 atmosphere, including the presence of a Ti adhesion layer (Supplementary Figs. S8 and S9).

Collectively, the exposure of graphene to H_2 molecules causes an increase in the interlayer distance of graphene, and molecular hydrogen is partially dissociated due to the existence of vacancy defects on graphene, as theoretically proposed. The dissociated H atoms are expected to be chemisorbed at the edge[30] and in the vacancies of the graphene[17,38], resulting in the *n*-type doping of graphene due to delocalised unpaired electrons.

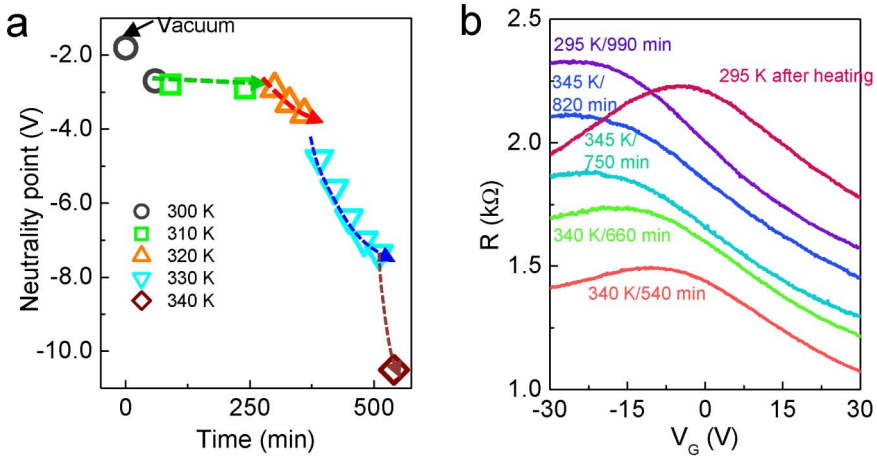

Figure 4 | V_G-dependent R as a function of temperature and exposure time for MLG at 10 bar of H_2 pressure. (a) The variation in CNP with respect to T and t. Upon exposure to 10 bar of H_2 pressure at 300 K, the CNP changes; it then changes slightly at 320 K and $t = 300$ min after exposure. Beyond 320 K/300 min, the slope of $\Delta V_{CNP}/\Delta t$ increases. (b) Beyond 340 K/540 min, the hole mobility decreases significantly and finally reaches zero. After heating to 393 K for 3 hr, the ambipolarity is restored.

Methods

Graphene samples were extracted from highly oriented pyrolytic graphite (HOPG) by mechanical exfoliation. The graphene samples were deposited on 300 nm SiO_2/highly *p*-doped Si wafers. The samples were selected by the colour contrast observed in optical microscopy images and characterised by micro-Raman spectroscopy (LabRam 300 with a 532 nm laser line of less than 1 mW, JY-Horiba) and AFM (SPA-400, Seiko instrument). A TEM investigation (HRTEM and diffraction pattern) of single-layer graphene was performed using an FEI Titan cube G2 60-300 installed at UNIST, equipped with an image aberration corrector. The microscope was operated at an accelerating voltage of 80 kV to reduce beam damage. Electrodes were fabricated by standard electron beam lithography (VEGA MM5150 with 30 keV filament, Tescan), the evaporation of Ti/Au (5/50 nm) and Cr/Au (10/40 nm) (ZZS550-2/D, Maestech), and lift-off procedures.

The devices were electrically characterised by a back gate sweep with a drain-source bias of V_{ds} = 1.0 or 2.0 mV using a semiconductor characterisation system (4200-SCS, Keithley) in a high-pressure chamber, which was completely made of stainless steel. The procedure is as follows. First, the devices were loaded into the chamber, which was evacuated at 393 K until the pressure reached approximately 10^{-6} Torr. Then, the graphene surfaces were exposed to 99.9999 % H_2 gas at pressures ranging from 1.0 to 25 bar.

1. Novoselov, K. S. *et al*. Electric field effect in atomically thin carbon films. *Science* **306**, 666–669 (2004).
2. Zhang,Y., Tan,Y.-W., Stormer, H. L. & Kim, P. Experimental observation of the quantum Hall effect and Berry's phase in graphene. *Nature* **438**, 201–204 (2005).
3. Geim, A. K. & Novoselov, K. S. The rise of graphene. *Nature Mater.* **6**, 183–191 (2007).
4. Nomura, K. & MacDonald, A. H. Quantum transport of massless Dirac fermions. *Phys. Rev. Lett.* **98**, 076602 (2007).
5. Lee, C., Wei, X., Kysar, J. W. & Hone, J. Measurement of the elastic properties and intrinsic strength of monolayer graphene. *Science* **321**, 385–388 (2008).
6. Elias, D. C. *et al*. Control of graphene's properties by reversible hydrogenation: evidence for graphane. *Science*, **323**, 610–613 (2009).
7. Balog, R. *et al*. Bandgap opening in graphene induced by patterned hydrogen adsorption. *Nature Mater.* **9**, 315–319 (2010).
8. Luo, Z. *et al*. Thickness-dependent reversible hydrogenation of graphene layers. *ACS Nano* **3**, 1781–1788 (2009).
9. Jaiswal, M. *et al*. Controlled hydrogenation of graphene sheets and nanoribbons. *ACS Nano* **5**, 888–896 (2011).
10. Ryu, S. *et al*. Reversible basal plane hydrogenation of graphene. *Nano Lett.* **8**, 4597–4602 (2008).
11. Deng, W.-Q., Xu, X. & Goddard, W. A. New alkali doped pillared carbon materials designed to achieve practical reversible hydrogen storage for transportation. *Phys. Rev. Lett.* **92**, 166103 (2004).
12. Patchkovskii, S. *et al*. Graphene nanostructures as tunable storage media for molecular hydrogen. *Proc. Natl. Acad. Sci. USA* **102**, 10439–10444 (2005).
13. Aga, R. S., Fu, C. L., Krčmar, M. & Morris, J. R. Theoretical investigation of the effect of graphite interlayer spacing on hydrogen absorption. *Phys. Rev. B* **76**, 165404 (2007).
14. Cabria, I., López, M. J. & Alonso, J. A. Hydrogen storage capacities of nanoporous carbon calculated by density functional and Møller-Plesset methods. *Phys. Rev. B* **78**, 075415 (2008).
15. Subrahmanyam, K. S. *et al*. Chemical storage of hydrogen in few-layer graphene. *Proc. Natl, Acad. Soc. USA*, **108**, 2674–2677 (2011).
16. Henwood, D. & Carey, J. D. Ab initio investigation of molecular hydrogen physisorption on graphene and carbon nanotubes. *Phys. Rev. B* **75**, 245413 (2007).
17. Allouche, A. & Ferro, Y. Dissociative adsorption of small molecules at vacancies on the graphite (0001) surface. *Carbon* **44**, 3320–3327 (2006).
18. Diño, W. A. *et al*. H_2 dissociative adsorption at the armchair edges of graphite. *Solid State Commun.* **132**, 713–718 (2004).
19. Tan, Y.-W. *et al*. Measurement of scattering rate and minimum conductivity in graphene. *Phys. Rev. Lett.* **99**, 246803 (2007).
20. Ferrari, A. C. & Robertson, J. Interpretation of Raman spectra of disordered and amorphous carbon. *Phys. Rev. B* **61**, 14095–14107 (2000).
21. Yan, J., Zhang, Y., Kim, P. & Pinczuk, A. Electric field effect tuning of electron-phonon coupling in graphene. *Phys. Rev. Lett.* **98**, 166802 (2007).
22. Pimenta, M. A. *et al*. Studying disorder in graphite-based systems by Raman spectroscopy. *Phys. Chem. Chem. Phys.* **9**, 1276–1291 (2007).
23. Barros, E. B. *et al*. Raman spectroscopy of graphitic foams. *Phys. Rev. B* **71**, 165422 (2005).
24. Ferrari, A. C. & Robertson, J. Resonant Raman spectroscopy of disordered, amorphous, and diamondlike carbon. *Phys. Rev. B* **64**, 075414 (2001).
25. Ristein, J., Stief, R. T., Ley, L. & Beyer, W. A comparative analysis of a-C:H by infrared spectroscopy and mass selected thermal effusion. *J. Appl. Phys.* **84**, 3836–3847 (1998).
26. Chen, J.-H. *et al*. Charged-impurity scattering in graphene. *Nature Phys.* **4**, 377–381 (2008).
27. Adam, S., Hwang, E. H., Galitski, V. M. & Das Sarma, S. A self-consistent theory for graphene transport. *Proc. Natl. Acad. Soc. USA* **104**, 18392–18397 (2007).
28. Sasa, T., Takahashi, Y. & Mukaibo, T. Crystal structure of graphite bromine lamellar compounds. *Carbon* **9**, 407–416 (1971).
29. Miura, Y., Kasai, H., Diño, W., Nakanishi, H. & Sugimoto, T. First principles studies for the dissociative adsorption of H_2 on graphene. *J. Appl. Phys.* **93**, 3395–3400 (2003).
30. Sha, X. & Jackson, B. The location of adsorbed hydrogen in graphite nanostructures. *J. Am. Chem. Soc.* **126**, 13095–13099 (2004).
31. Ao, Z. M. & Peeters, F. M. Electric field activated hydrogen dissociative adsorption to nitrogen-doped graphene. *J. Phys. Chem. C* **114**, 14503–14509 (2010).
32. McKay, H., Wales, D. J., Jenkins, S. J., Verges, J. A. & de Andres, P. L. Hydrogen on graphene under stress: molecular dissociation and gap opening. *Phys. Rev. B* **81**, 075425 (2010).
33. Banhart, F., Kotakoski, J. & Krasheninnikov, A. V. Structural defects in graphene. *ACS Nano* **5**, 26–41 (2011).
34. Boukhvalov, D. W., Katsnelson, M. I. & Lichtenstein, A. I. Hydrogen on graphene: electronic structure, total energy, structural distortions and magnetism from first-principle calculations. *Phys. Rev. B* **77**, 035427 (2008).
35. Boukhvalov, D. W. & Katsnelson, M. I. Chemical functionalization of graphene with defects. *Nano Lett.* **8**, 4373–4379 (2008).
36. Vergés, J. A. & de Andres, P. L. Trapping of electrons near chemisorbed hydrogen on graphene. *Phys. Rev. B* **81**, 075423 (2010).
37. Brenner, K., Yang, Y. & Murali, R. Edge doping of graphene sheets. *Carbon* **50**, 637–645 (2012).
38. Bae, G., Cha, J., Lee, H., Park, W. & Park, N. Effects of defects and non-coordinating molecular overlayers on the work function of graphene and energy-level alignment with organic molecules. *Carbon* **50**, 851–856 (2012).

Acknowledgements

We thank K. S. Novoselov, P. Kim, and C. N. R. Rao for helpful discussions and comments and H.J. Kim for supporting the manufacture of the high-pressure chamber. N.P. was supported by the Hydrogen Energy R&D Center, a 21st Century Frontier R&D Program funded by the Ministry of Science and Technology of Korea. Y.W.P. acknowledges support from the GRDC (2009-00514) through the Ministry of Education, Science and Technology (MEST), Korea. S.W.L. acknowledges support from the WCU program of the MEST (R31-2008-000-10057-0) and from the NRF (2011-0021207). Y. J. acknowledges support from MEST (20120002424, 2012K001288).

Author contributions

B.H.K. and S.J.H. designed the study, performed experiments, collected and analysed data, and wrote the paper. S.J.B., M.P., S.W.C., J.L., and J.C.L. performed the experiments. H.Y.J. performed and analysed the TEM study. N.P. and M.L. provided the theoretical analysis. S.W.L. provided bilayer graphene and analysed the data. H.S.S. analysed the data and edited the manuscript. Y.J. and Y.W.P. supervised the study and wrote the paper. All authors discussed the results and commented on the manuscript.

Additional information

Supplementary information accompanies this paper at http://www.nature.com/scientificreports

Competing financial interests: The authors declare no competing financial interests.

How to cite this article: Kim, B.H. *et al*. *N*-type graphene induced by dissociative H_2 adsorption at room temperature. *Sci. Rep.* **2**, 690; DOI:10.1038/srep00690 (2012).